



## ***Arundo donax L.* as a low-cost and promising biosorbent for the removal of crystal violet from aqueous media: kinetic, isotherm and thermodynamic investigations**

Fouad Krika<sup>a,\*</sup>, Abderezak Krika<sup>b</sup>, Ahmed Azizi<sup>c</sup>

<sup>a</sup> Laboratoire d'étude sur les interactions matériaux-environnement (LIME), Faculté des sciences et de la technologie, Université de Jijel, BP 98 Ouled Aissa, Jijel, 18000, Algérie

<sup>b</sup> Department of Environmental Sciences and Agronomic Sciences, Faculty of Nature Life and Sciences, University of Jijel BP 98 Ouled Aissa, Jijel 18000, Algeria

<sup>c</sup> Department of Process Engineering, Faculty of Technology, University of Amar Telidji, BP 37G, Laghouat, 03000, Algeria

### ARTICLE INFO

### ABSTRACT

#### Article history:

Received

Received in revised form

Accepted

Available online

#### Keywords:

Adsorption

Crystal violet

Isotherms

Kinetics

Thermodynamics

In the present study, *Arundo donax L.* was used as a low-cost biosorbent for the uptake of basic dye crystal violet (CV) from aqueous media. Systematic batch mode studies of adsorption of crystal violet (CV) on *Arundo donax L.* were carried out as a function of process of parameters includes initial CV concentration, dose of adsorbent, pH, contact time and temperature. The equilibrium adsorption data were analyzed by Langmuir, Freundlich, Temkin and Dubinin–Radushkevich (D-R) isotherm models. The adsorption of CV followed the Langmuir model with a maximum adsorption capacity ( $q_{max}$ ) of 19.60 mg/g and pseudo second-order kinetics under a specified set of conditions. The thermodynamic parameters like free energy ( $\Delta G^\circ$ ), enthalpy ( $\Delta H^\circ$ ) and entropy ( $\Delta S^\circ$ ) changes for the adsorption of CV ions have been evaluated and it has been found that the reaction was spontaneous and exothermic in nature.

Owing to its rapid adsorption rate and uptake capacity, stem of *Arundo donax L.* seems to be a promising biosorbent for removal of toxic dyes from wastewater.

### 1. Introduction

Dyes are used in large quantities in many industries including textile, leather, cosmetics, paper, printing, plastic, pharmaceuticals, food, etc [1]. To color their products, this generates wastewater characteristically high in color [2]. Currently, over than 100.000 dyes are commercially available and more than  $8 \times 10^5$  tons are produced annually to supply these industries [3].

Discharging of dye-containing effluents into hydrosphere is prohibited not only because of their color, which reduces the sunlight penetration into the water, but also because of toxic, carcinogenic and mutagenic nature of their breakdown products [4]. As a typical cationic dye, crystal violet (CV) belongs to triphenylmethane group, and is widely applied in coloring paper, temporary hair colorant, dyeing cottons, and wools. CV is harmful by inhalation, ingestion and skin contact, and has also been found to cause cancer and severe eye irritation to human beings [5,6]. As such, a method for efficiently removing CV molecules from wastewaters is urgently-needed.

Many physical and chemical processes [7] have been used to remove synthetic dyes from industrial wastewaters such as coagulation-flocculation[8], membrane filtration[9], Fenton process [10], Photocatalytic degradation[11], irradiation[12], ozonation[13] and adsorption[14]. Among these methods, adsorption has been extensively employed for the removal of dye molecules from different types of water due to its easy operational conditions, low cost, simple design and high efficiency [15]. Activated carbon is the most efficient adsorbent used to date, but its high cost limits its applicability. Research is currently focusing on the use of low cost commercially available organic materials as viable substitutes for activated carbon; in fact, Lignocellulosic materials exhibit interesting capacities as pollutant adsorbents.

*Arundo donax L.*, belonging to the grass family, is distributed from the Mediterranean region to China and Japan. It is a fast growing perennial grass. Under optimum conditions it can attain growth rate of 0.7 m per week or 10 cm per day, among the fastest growth rate in plants [16]. In addition, it contains high

amount of lignin and cellulose therefore it is an energy crop, which displays many attractive characteristics for the production of biomass [17,18], of pulp and paper [19] and of activated carbons [20]. Also, that species could be used as biofiltering material for sewage effluent treatment [21] and has been found the capability of accumulate heavy metals to its body [22].

Considering these facts presented above, *Arundo donax L.* could be a non-living biomass with adsorptive properties which can be explored to remove pollutants from water. Our recent findings have shown that the stem of *Arundo donax L.* was able to remove heavy metals [23]. As an extension to this finding, we explore the possibility of the potential utilization of the stem of *Arundo donax L.* as means to remove toxic dyes from aqueous solutions. To the best of our knowledge, there have been no reported studies on the use of *Arundo donax L.* for the removal of toxic dyes. The objective of this paper is to examine the adsorption of CV on stem of *Arundo donax*.

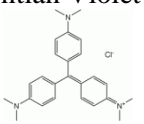
This research study is conducted to utilize the *Arundo donax L.* stem as a potential adsorbent to remove crystal violet from its aqueous solutions. Removal efficiency was tested with a series of batch experiments that varied solution pH, adsorbent dosage, contact time, initial dye concentration and temperature. Removal mechanisms are discussed via FTIR,  $pH_{pzc}$  analyses and Boehm titration method. The equilibrium isotherms, kinetics, and thermodynamic parameters were determined to predict the nature of CV adsorption.

## 2. Materials and methods

### 2.1. Chemicals

All reagents, supplied by Merck-India, were of analytical reagent grade and used as received. Physico-chemical characteristics of CV are given in Table 1.

**Table 1.** Physicochemical characteristics

Dye	Crystal violet
C.I. number	42555
C.I. name	Basic Violet 3
Class	triarylmethane
Molecule weight (g/ mol)	407.99
Chemical formula	$C_{25}H_{30}ClN_3$
Water solubility (g/L)	16 (25°C)
$\lambda_{max}$ (nm)	590
Synonyms	Basic Violet 3, Gentian Violet
Molecular structure	

A stock solution of the dye containing 1000 mg/L was prepared by dissolving the required amount of dye in double distilled water. Solutions of different concentrations used in the further experiments were prepared by diluting the stock solution. The initial pH of the solution was adjusted using 0.1M HCl and 0.1M NaOH solutions.

### 2.2. Adsorbent preparation

The *Arundo donax L.* used in this study was obtained from an agricultural area in El kanar, Jijel, Algeria in February 2018. The collected biomaterial was extensively washed with tap water to remove soil and dust and then cut to select stems out. The stems were dried by exposure to the sunlight for 3 days and subsequently at 80°C for 3h in a hot air convection oven. The samples were then ground in a mortar and sieved till finally became homogenous powder, yielding size fractions between 80 and 100 mesh.

### 2.3. Adsorbent characterization

The functional groups of *Arundo donax L.* were determined using Shimadzu IR 8400s spectrophotometer for Fourier transform infrared spectroscopy (FTIR) analysis using KBr disc method. The point zero charge ( $pH_{pzc}$ ) was used to determine the point where the density of electrical charge is zero. The solid addition method [24] was used to determine the point zero charge of the adsorbent. The surface acidic and basic function groups were determined by Boehm titration method [25].

### 2.4. Analytical method

The equilibrium/residual concentrations of CV in solutions were determined with the help of a Shimadzu spectrophotometer (6101-UV-VIS). All measurements were performed at the maximum absorbency visible wave length. The absorption spectrum of the dye was recorded between the wavelength ranges of 250-750 nm. As can be seen on Fig. 01, the maximal wavelength of CV was 485 nm.

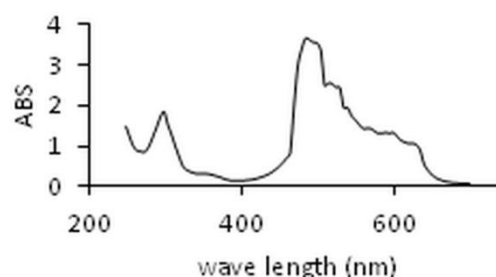


**Figure 1.**  $\lambda_{max}$  of CV

### 2.6. Batch adsorption studies

Batch adsorption experiments were carried out to understand the effects of solution pH, adsorbent dosage, contact time, initial dye concentrations and

temperature. The dye adsorption was performed in a set of adsorbent for a specific period of contact time in an orbital shaker. When it reached equilibrium, the solution was centrifuged at 3000 rpm for 10 min, the absorbance of supernatants was determined by spectrophotometer, and then, the final concentration

was measured. The adsorption capacity  $q_e$ (mg/g) and removal efficiency (%) were calculated as follows:

$$q_e = \frac{(C_0 - C_e) \cdot V}{m} \quad (1)$$

$$\% \text{Removal} = \frac{(C_0 - C_e)}{C_0} \cdot 100 \quad (2)$$

Where  $C_0$  and  $C_e$  are the initial and final dye concentration (mg/L),  $V$  is the volume of the dye solution (L) and  $m$  is the mass of adsorbent (g).

## 2.6. Adsorption kinetic and isotherm models

In order to study the adsorption of CV onto *Arundo donax L* and to interpret the results, experimental data obtained were fitted to different kinetic models such as the pseudo-first-order[26], the pseudo-second order [27]. To establish the rate determining steps for CV dye adsorption, the kinetic data were further analyzed by the intraparticle diffusion model [28].

The purpose of the adsorption isotherms is to relate the adsorbate concentration in the bulk and the adsorbed amount at the interface [29]. Thus, isotherm modeling is important for adsorption data interpretation and prediction. The equilibrium characteristics for CV ions adsorption on *Arundo donax L* were evaluated by Langmuir, Freundlich, Dubinin-Radushkevich and Temkin isotherms. All kinetic and isotherm models were fitted to experimental data using their non-linear equations (Table 2).

## 3. Results and discussion

### 3.1. Adsorbent characterization

**Table 2.** Non-linear equations of kinetic and isotherm models

Kinetic models	
Pseudo-first order	$q_t = q_e(1 - e^{-k_1 t})$
Pseudo-second order	$q_t = \frac{k_2 q_e^2 t}{1 + k_2 q_e t}$
Intraparticle diffusion	$q_t = k_{id} t^{0.5} + C$
Isotherm models	
Langmuir	$q_e = \frac{q_{max} K_L C_e}{1 + K_L C_e}$
Freundlich	$q_e = K_F C_e^{1/n}$
	$q_e = Q_m \exp(-\beta \varepsilon^2)$
Dubinin-Radushkevich	$\varepsilon = RT \ln(1 + \frac{1}{C_e})$
	$E = \frac{1}{\sqrt{2\beta_{DR}}}$
Temkin	$q_e = \frac{RT}{B_T} \log A_T C_e$

$k_1$  ( $\text{min}^{-1}$ ) = rate constant of pseudo-first order;  $k_2$  ( $\text{g/mg min}$ ) = rate constant of pseudo-second order;  $k_{id}$  ( $\text{mg g}^{-1} \text{min}^{-0.5}$ ) = intraparticle diffusion rate constant;  $q_{max}$  ( $\text{mg/g}$ ) = maximum adsorption capacity;  $K_L$  ( $\text{L/mg}$ ) = Langmuir constant;  $K_F$  ( $(\text{mg/g}) (\text{L/mg})^{1/n}$ ) = Freundlich constant;  $n$  = Freundlich exponent;  $\beta_{DR}$  ( $\text{g}^2/\text{J}$ ) = activity coefficient;  $\varepsilon$  ( $\text{J/g}$ ) = Polanyi potential;  $B_T$  ( $\text{J/mol}$ ) = Temkin constant;  $A_T$  ( $\text{L/mg}$ ) = maximum binding constant;  $R$  = universal gas constant ( $8.314 \text{ J/mol K}$ );  $T$  = absolute temperature (K);  $E$  ( $\text{J/mol}$ ) = mean free energy of sorption.

#### 3.1.1. FTIR analysis

FTIR spectrum study was carried out to explain the adsorption mechanism for identifying the presence of functionalities of the *Arundo donax L* biomass and analyte.

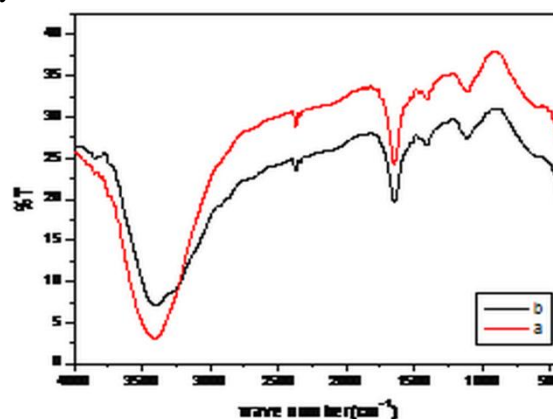


**Figure 2.** FTIR spectra of *Arundo donax L* (a) untreated (b) after adsorption with CV.

The FTIR spectrum of *Arundo donax* and CV-loaded *Arundo donax L* (Fig. 2a and b) revealed that upon treatment of adsorbent with CV, the wavelength of the broad band at  $3,406\text{ cm}^{-1}$  is decreased to  $3,396\text{ cm}^{-1}$  indicating that hydroxyl and amino groups are involved in bond formation with dye. A significant decrease in wavelength is observed for C=O stretching of the carboxylic acid peak from  $1,652\text{ cm}^{-1}$  to  $1,636\text{ cm}^{-1}$ , indicating that carboxylic acid groups play a significant role in the adsorption of CV by *Arundo donax L*.

### 3.1.2. Boehm titration

Boehm titration method was used to determine the surface chemistry and the amount of functional groups such as phenolic, lactonic, and carboxylic groups of *Arundo donax L*. Surface functional groups (Table 3) clearly indicates that the total acidic groups are highly greater (1.306 meq/g), indicating the *Arundo donax L* surface is acidic, which resulted from the presence of major acidic groups.

**Table 3.** Boehm results of *Arundo donax*

Active sites	Meq/g
Total acidic sites	1.306
Carboxylic	0.548
Lactone	0.130
Phenolic	0.626
Total basic sites	0.09

### 3.2. Effect of initial pH

Medium pH plays a significant role in the uptake of adsorbates by biosorbents as the pH would cause the surface charge to alter, thereby affecting the efficiency of biosorbents [30].

The pH at the point of zero charge ( $\text{pH}_{\text{PZC}}$ ) was used to characterize the properties of the *Arundo donax L* surface. Thus, When solution  $\text{pH} < \text{pH}_{\text{PZC}}$ , the surface of the adsorbent is predominately positive whereas when solution  $\text{pH} > \text{pH}_{\text{PZC}}$ , the adsorbent's surface will be predominately negative. Therefore, the adsorption of cationic species such as CV is favored under the latter condition.

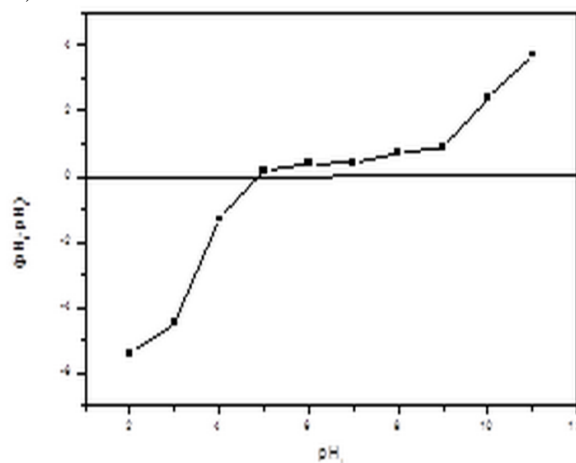


**Figure 3.** Determination of  $\text{pH}_{\text{PZC}}$  of the *Arundo donax L*.

The result in Fig. 3 shows that the surface charge of *Arundo donax L* at  $\text{pH} 4.9$  was zero. Hence, the  $\text{pH}_{\text{PZC}}$  of adsorbent was 4.9.

Fig. 4 shows the adsorption of CV as a function of solution pH from 3 to 8. The adsorption capacity of *Arundo donax L* was highest (18.42 mg/g) at a pH value of 3; when the  $\text{pH}$  was increased to 8, the adsorption capacity decreased to 13.28 mg/g but still did not reach equilibrium.

According to the concept of  $\text{pH}_{\text{PZC}}$ , at  $\text{pH} > 4.9$  where the dye adsorption should be higher due to predominately negatively charged surface thus favoring the adsorption of cationic dye molecules via electrostatic attraction, however experimental data for CV showed otherwise. This disagreement with  $\text{pH}_{\text{PZC}}$  concept merely indicated that the adsorption of CV is not occurring purely by electrostatic interaction, while other attractive forces such as hydrophobic–hydrophobic interaction and hydrogen bonding may be significantly dominant. This behaviour was also observed by [31, 32].

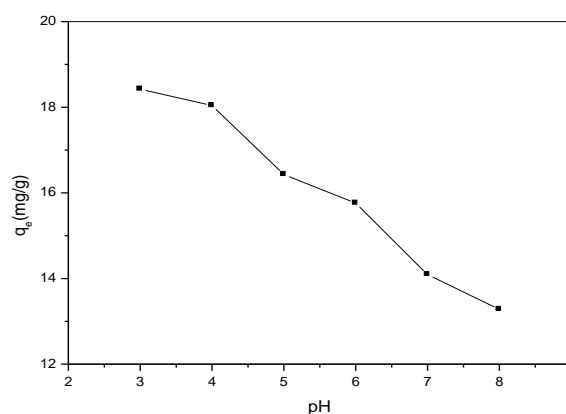


**Figure 4.** Effect of pH on the adsorption of CV onto *Arundo donax* ( $C_0 = 100\text{ mg/L}$ ,  $m = 1\text{ g}$ ,  $T = 25^\circ\text{C}$  and contact time = 240 min).

### 3.3. Effect of adsorbent dose

One of the parameters that strongly affect the adsorption removal is the dose of the adsorbents [33]. The effect of adsorbent dose on the removal of CV by *Arundo donax L* at initial concentration ( $C_0=100$  mg/L) is illustrated in Fig. 5.

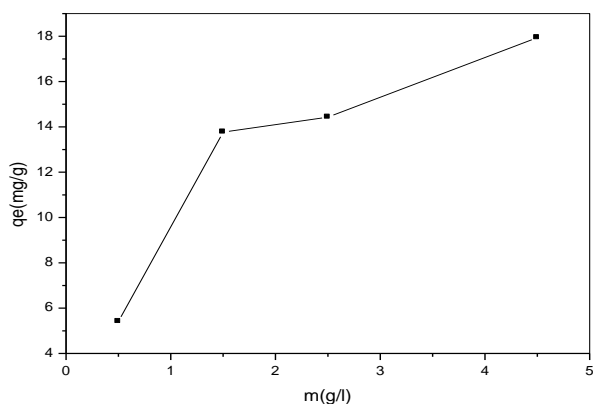


**Figure 5.** Effect of adsorbent dosage on CV removal by *Arundo donax L* ( $C_0=100$  mg/L, pH = 3, T = 25°C and contact time = 240 min).

With increase in adsorbent dose, from 0.5 g/L to 4.5 g/L, the amount of adsorbed CV increases from 5.41 mg/g to 17.94 mg/g and maximum amount removal was observed at adsorbent dose of 4.5 g/L where the quantity removal was 17.94 mg/g. This pattern is due to the availability of active sites or surface area on the adsorbent increases with increase of adsorbent dosage facilitates the adsorption of the CV which in turn results in increase of amount removal [34].

### 3.4. Effect of ionic strength

Generally, most of dying processes utilized in their industries large amounts of salts. Adsorption process can be affected by the presence of some metal ions which are present in wastewaters as ionic strength can affect electrostatic and hydrophobic–hydrophobic interactions. Both electrostatic attraction and repulsion are important for the adsorption. Electrostatic attraction promotes the adsorption; on the contrary, electrostatic repulsion suppresses the adsorption [35]. Fig. 6 presents the effect of ionic strength on the uptake of CV.

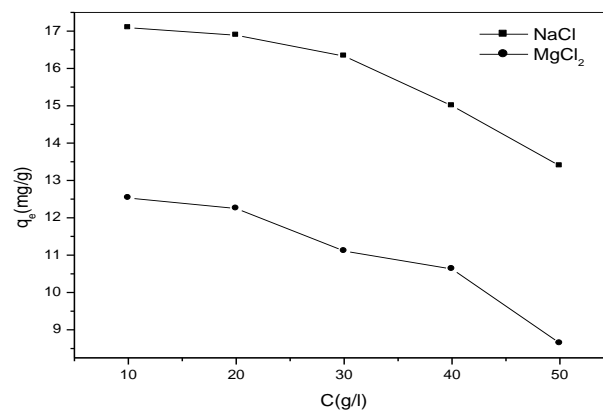


**Figure 6.** Effect of salts concentration for CV adsorption on *Arundo donax L* ( $C_0=100$  mg/L,  $m=4.5$  g/L, contact time = 120 min, pH 3).

It was observed that for both salts, adsorption amount decreased with increase in ionic strength. As NaCl concentration changed from 10 to 50 g/L, the removal of CV decreased by 3.7% (from 17.09% to 13.39%, Fig. 5), while the uptake of CV decreased by 3.89% (from 12.63% to 8.64%, Fig. 6) as MgCl<sub>2</sub> concentration varied from 10 g/L to 50 g/L.

This behavior is usually observed for the removal of dyes and has been reported in many studies [36]. This reduction in dye uptake at high salt concentration suggested that electrostatic interaction is not the major force of interaction but hydrophobic–hydrophobic interaction and other forces [32].

### 3.5. Adsorption kinetics

The adsorption kinetic is one of the most important properties in defining the rate and mechanism of the adsorption process [37]. Fig. 7 depicts the adsorption of CV dye as a function of contact time using three initial dye concentrations (100, 200 and 300 mg/L). The plots show that equilibrium was achieved within 30 minutes indicating *Arundo donax* was an effective adsorbent for the short contact time with the CV.

The time variation plot indicates that the removal of dye is rapid in initial stages but when it approaches equilibrium, it slows down gradually. The fast adsorption at the initial stage may be due to the fact that a large number of surface sites are available for adsorption but after a lapse of time, the remaining surface sites are difficult to be occupied. This is because of the repulsion between the solute molecules of the solid and bulk phases, thus, make it take long time to reach equilibrium [38].

kinetic parameters obtained for CV adsorption are listed in Table 4.

The results show (Table 4, Fig. 8a, b and c) for pseudo-

$C_0$ (mg/L)	$q_{e,exp}$ (mg/L)	Pseudo-first order			Pseudo-second order			Intraparticle diffusion		
		$k_1$	$q_e$	$R^2$	$k_2$	$q_e$	$R^2$	$K_{id}$	$q_e$	$R^2$
100	16.80	0.213	3.20	0.804	0.037	16.66	0.999	1.21	6.05	0.78
200	38.51	0.089	90.9	0.834	0.033	38.46	1	5.19	34.81	0.64
300	58.21	0.071	16.44	0.821	0.015	58.82	0.999	7.75	73.52	0.847

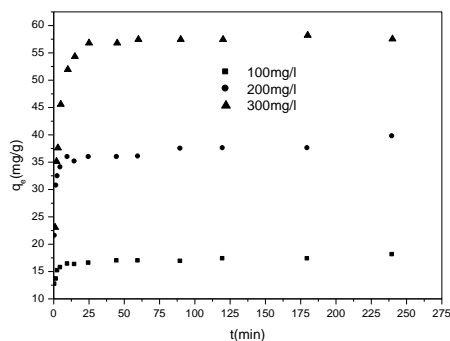


**Figure 7.** Effect of initial dye concentration and contact time on CV removal by *Arundo donax L* (pH 3,  $m = 4.5$  g/L and  $T = 298$  K).

When the initial dye concentration increased from 100 mg/L to 300 mg/L the adsorption capacity increased from 17.28 mg/g to 58.21 mg/g. This is due to increase in the driving force of the concentration gradient, as an increase in the initial concentration. The concentration provides an important driving force to overcome all mass transfer resistance of the dye between the aqueous and solid phases. Hence a higher initial concentration of dye will enhance the adsorption process [39]. The

first kinetic model that the values of  $R^2$  were low and the experimental  $q_{e,exp}$  values do not agree well with the calculated values

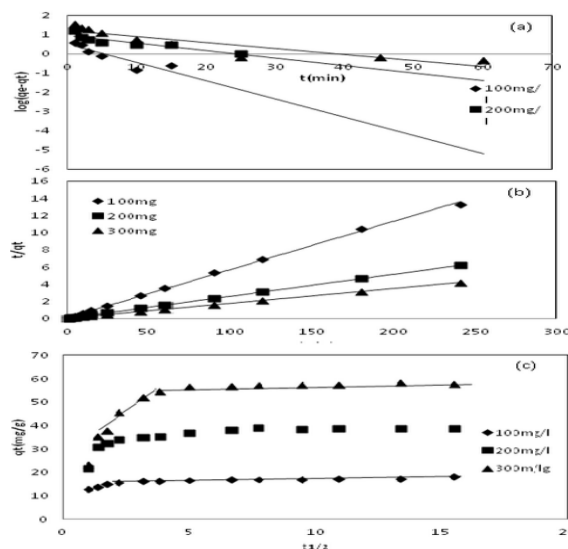


**Figure 8.** Kinetics plots for the adsorption of CV onto *Arundo donax L*: (a) pseudo-first order, (b): pseudo-second order, (c): intraparticle diffusion.

**Table 4.** Parameters of the kinetic models for CV adsorption by *Arundo donax*.

This shows that the adsorption of CV onto *Arundo donax L* is not first-order kinetic, indicating that the adsorption was not diffusion-controlled and adsorption was not preceded by diffusion through a boundary [40]. This is confirmed by results obtained with the intraparticle model. In this model, the plot of  $q_t$  versus  $t^{1/2}$  were not linear over the whole time range. Furthermore, it may be seen that the intra-particle diffusion of CV dye occurred in 2 stages. The first straight portion indicates that boundary layer diffusion probably limited CV adsorption [41] and the second linear portion is attributed to intra-particle diffusion. The correlation coefficient values for the pseudo-second order rate equation ( $R^2 = 0.9993 - 0.9999$ ) (Table 4, Fig. 8b) were found to be higher than the pseudo-first order rate equation ( $R^2 = 0.9653 - 0.9451$ ) and the  $q_{e,calc}$  and  $q_{e,exp}$  values were in close agreement with each other for pseudo-second order model, which conformed that the adsorption process followed the pseudo-second order kinetic model [29].

### 3.6. Adsorption isotherms

The purpose of the adsorption isotherms is to relate the adsorbate concentration in the bulk and the adsorbed amount at the interface [42]. The non-linear isotherm models of Langmuir, Freundlich, Dubinin-Radushkevich(D-R) and Temkin were adjusted to experimental data and they are shown in Fig. 9.

The Langmuir model [43] is based on the assumption that the maximum adsorption occurs when a saturated monolayer of solute molecules is present on the adsorbent surface, the energy of adsorption is constant and there is no migration of adsorbate molecules in the surface plane.

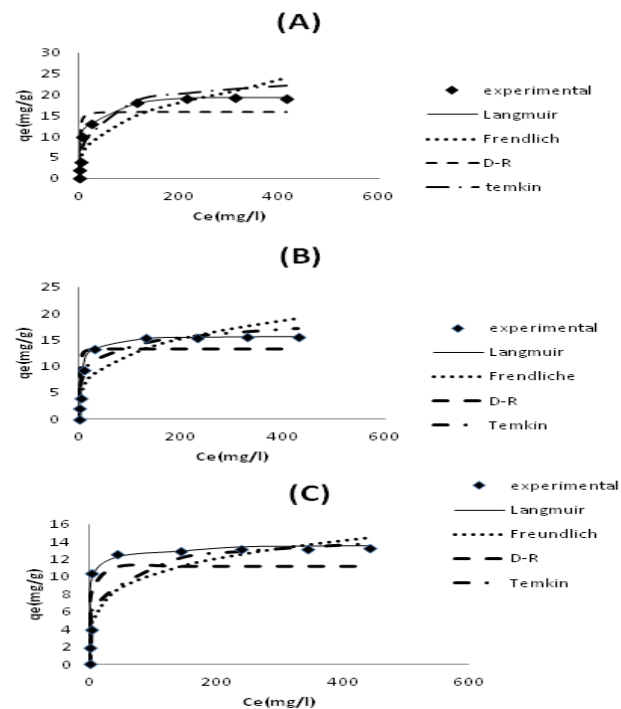
The Freundlich isotherm model [44] is the earliest known relationship describing the non-ideal and reversible adsorption, which can be applied to multilayer adsorption, on the basis of an assumption concerning the energetic surface heterogeneity. The Freundlich adsorption capacity magnitude ( $n$ ) is useful to assess the favorability of the adsorption. The  $n$  values between 2-10 indicate high adsorption capacity, whereas  $n$  values between 1-2 indicate moderate adsorption

capacity, and n values lower than 1 suggest a poor adsorption capacity.

Temkin [45] considered the effects of some indirect adsorbate/adsorbate interactions on adsorption isotherms and suggested that because of these interactions the heat of adsorption of all the molecules in the layer would decrease linearly with coverage.

The Dubinin-Redushkevich [46] is an empirical equation which is applied to distinguish between physical and chemical adsorption. The  $\beta_{D-R}$  is the activity coefficient related to mean adsorption energy and E is the mean free energy, which can be calculated by using  $\beta_{D-R}$  values. For magnitude of E between 8 KJ/mol and 16KJ/mol, the adsorption process followed chemical ion exchange, and values of E below 8 KJ/mol were the characteristic of physical adsorption process [47].

The parameters obtained for each model and their correlation coefficients are displayed in Table 5. High  $R^2$  are derived by fitting experimental data into the Langmuir isotherm model ( $R^2 > 0.99$ ) as compared with the Freundlich ( $R^2 > 0.63-0.87$ ), Dubinin-Radushkevich ( $R^2 > 0.85- 0.97$ ) and Temkin ( $R^2 > 0.64-0.86$ ) isotherm models.



T(K)	$\Delta G^0$ (KJ/ mol)	$\Delta S^0$ (J/ mol K)	$\Delta H^0$ (kJ/ mol)	$R^2$
298	-07.31			
308	-08.10	-89.08	-18.98	0.999
318	-09.41			

Figure 9. Isotherms of CV) adsorption by Arundo donax as a function of temperatures: (A ): 25°C, (B): 35°C and (C): 45°C

High  $R^2$  are derived by fitting experimental data into the

Freundlich ( $R^2 > 0.63-0.87$ ), Dubinin-Radushkevich ( $R^2 > 0.85- 0.97$ ) and Temkin ( $R^2 > 0.64-0.86$ ) isotherm models.

Table 5. Parameters for adsorption of CV on Arundo donax L for various isotherm models

Isotherm models	25°C	35°C	45°C
<b>Langmuir</b>			
$q_{max}$ (mg/g)	19.60	15.87	12.65
$K_L$ (L/ mg)	0.228	0.205	0.439
$R^2$	0.999	0.999	0.998
<b>Freundlich</b>			
$K_F$ (mg/g)(L/mg) <sup>1/n</sup>	3.13	3.10	3.56
n	3.01	3.23	4.18
$R^2$	0.874	0.800	0.630
<b>Dubinin-Raduschkevich(D-R)</b>			
$q_{max}$ (mg/g)	15.81	13.31	13.14
$B_{DR}$	$7.10^{-7}$	$8.10^{-7}$	$10^{-6}$
E(KJ/ mol)	0.85	0.79	0.71
$R^2$	0.808	0.857	0.973
<b>Temkin</b>			
$A_T$ (L/ mg)	5.023	4.172	30.03
$B_T$	2.778	2.299	1.454
$R^2$	0.811	0.862	0.640

Langmuir model (R<sup>2</sup> > 0.99) as compared with the Freundlich (R<sup>2</sup> > 0.63-0.87), Dubinin-Radushkevich (R<sup>2</sup> > 0.85- 0.97) and Temkin (R<sup>2</sup> > 0.64-0.86) isotherm models.

The *Arundo donax L* showed maximum monolayer adsorption capacity ( $q_{max}$ ) for CV of 19.60 mg/g. This finding was compared to other studies on the adsorption of CV on different adsorbents (Table 6). The most important parameter to compare is the Langmuir  $q_{max}$  value since it is a measure of adsorption capacity of the adsorbent. The value of  $q_{max}$  in this study is larger than those in most of previous works. This suggests that CV could be easily adsorbed on *Arundo donax L*.

**Table 6.**  $q_{max}$  of various adsorbents

Adsorbents	$q_{max}$ (mg/g)	References
<i>Arundo donax</i>	<b>19.60</b>	<b>This work</b>
Orange peel	11.50	[48]
Banana peel	12.20	[48]
peat	8.20	[49]
Calotropis procera leaf	4.10	[50]
Citrullus lanatus rind	12.10	[51]
Nanomagnetic iron oxid	12.70	[52]
Chitosan	28.5	[53]
Water hyacinth	322.58	[54]
Magnetically modified activated carbon	67.10	[52]

### 3.7. Thermodynamic studies

The effect of a change in temperature on the CV-*Arundo donax L* adsorption system was studied to determine the thermodynamic parameters and to investigate the nature of the process. The change in Gibbs free energies ( $\Delta G^\circ$ ) was calculated with equation 3.  $\Delta H^\circ$  and  $\Delta S^\circ$  were calculated from the slope and intercept of the plot of  $\ln K_d$  versus  $1/T$  using Van't Hoff equation 4 (data not shown):

$$\Delta G = -RT \ln K_d \quad (3)$$

$$\ln K_d = \frac{\Delta S^\circ}{R} - \frac{\Delta H^\circ}{RT} \quad (4)$$

Where  $R$  is the universal gas constant (8.314 J/mol K),  $T$  is the temperature of the medium (K) and  $K_d$  is the distribution coefficient. It is determined from:

$$K_d = \frac{q_e}{C_e} \quad (5)$$

All the thermodynamic parameters are listed in Table 7

**Table 7.** Thermodynamic parameters of the CV Adsorption onto *Arundo donax L*

The negative value of  $\Delta H^\circ$  shows that the adsorption of CV on *Arundo donax* is exothermic

process. The negative value of  $\Delta S^\circ$  indicates the decreased disorder and randomness at the solid solution interface of CV with adsorbent. The negative values of  $\Delta G^\circ$  indicate the adsorption is favorable and spontaneous.  $\Delta G^\circ$  values decreases with increase in temperature. The decrease in the value of  $\Delta G^\circ$  with temperature further showed the decrease in feasibility of adsorption at elevated temperatures. The change in free energy for physisorption is between -20 and 0 KJ/mol, but chemisorption is in a range of -80 to -400 KJ/mol [55]. The values of  $\Delta G^\circ$  obtained in this study are within the ranges of -20 and 0 KJ/mol, indicating that the physisorption is the dominating mechanism.

### 4. Conclusion

In the present investigation, *Arundo donax L* was considered as cheap adsorbent for the retention of crystal violet (CV) from aqueous media. The operational parameters, including: surface chemistry, solution pH, adsorbent dosage, isotherm models, adsorption kinetics, and thermodynamics were studied to investigate the adsorption process. FTIR spectroscopy showed that the carboxylic acid groups play a significant role in the adsorption of CV by *Arundo donax L*.

The experimental results show that the optimum conditions of adsorption were pH3.0, adsorbent dosage 4.5 g/L at 298K for 60 min. The adsorption process was not severely affected by high ionic strength. The equilibrium data were correlated reasonably well by Langmuir adsorption isotherm. The maximum adsorption capacity of 19.60 mg/g was exhibited by *Arundo donax L*. Kinetics of adsorption of CV was fast and followed the pseudo-second-order. Thermodynamic studies showed that adsorption CV-*Arundo donax* system is spontaneous and exothermic. Thus, it can be concluded that the biomaterial *Arundo donax* biomass can be used as excellent sorbent for the removal of dyes from wastewater.

### References

- [1] F.Z. Benhachem, T. Attar, F. Bouadbdallah. Kinetic study of adsorption methylene blue dye from aqueous using activated carbon from starch. *Chem.Rev. Lett.*, 2(2019) 33-39.
- [2] S.S. Azhar, A.G. Liew, D. Suhardy, K.F. Hafiz, M.D.I. Hatim. Dye removal from aqueous solution by using adsorption on treated sugarcane bagasse. *Am. J. Appl. Sci.*, 200(2005) 1499-1503.
- [3] M.X Wang., Q.L.Zhang, S.J. Yao, A novel biosorbent formed of marine-derived *Penicillium janthinellum* mycelial pellets for removing dyes from dye-containing wastewater. *Chem. Eng. J.*, 259 (2015)837-844.
- [4] S.Wang, Y. Boyjoo, A. Choueib, Z.H.U. Zhu, Removal of dyes from aqueous solution using fly ash and red mud. *Water Res.*, 39 (2005) 129-138.
- [5] Y. Lin, X. He, G.Han, Q. Tian, W. Hu, Removal of crystal violet from aqueous solution using powdered mycelial biomass of *Ceriporia lacerata* P2. *J. Environ. Sci.*, 23(2011) 2055-2062.



- [6] Saeed, M. Sharif, M. Iqbal, Application potential of grapefruit peel as dye sorbent: kinetics, equilibrium and mechanism of crystal violet adsorption. *Bioresour. Technol.*, 179(2010) 564-572.
- [7] U.A. Guler, M. Ersan, E. Tuncel, F. Dügenci, Mono and simultaneous removal of crystal violet and safranin dyes from aqueous solutions by HDTMA-modified *Spirulina* sp. *Process Saf. Environ. Prot.*, 99(2016)194-206.
- [8] Szyguła, E. Guibal, M. Arino Palacín, M. Ruiz, AM. Sastre, Removal of an anionic dye (Acid Blue 92) by coagulation–flocculation using chitosan. *J. Environ. Manag.*, 90(2009) 2979-2986.
- [9] E. Alventosa-de Lara, S. Barredo-Damas, M.I. Alcaina-Miranda, MI. Iborra-Clar, Ultra filtration technology with a ceramic membrane for reactive dye removal: optimization of membrane performance. *J. Hazard. Mater.*, 209-210(2012) 492-504.
- [10] M. Karatas, Y.A.Argun, M.E.Argun, Decolorization of antraquinonic dye, Reactive Blue 114 from synthetic wastewater by Fenton process: Kinetics and thermodynamics. *J. Ind. Eng. Chem.*, 18(2012) 1058-1062.
- [11] T.A. Saleh, V.K. Gupta, Photo-catalyzed degradation of hazardous dye methyl orange by use of a composite catalyst consisting of multi-walled carbon nanotubes and titanium dioxide. *J. Colloid Interface Sci.*, 371(2012) 101-106.
- [12] J.Paul, K.P.Rawat, K.S.S.Sarma, S. Sabharwal, Decoloration and degradation of Reactive Red-120 dye by electron beam irradiation in aqueous solution. *Appl. Radiat. Isot.*, 69(2011) 982-987.
- [13] G. Moussavi, M. Mahmoudi, Degradation and biodegradability improvement of the reactive red 198 azo dye using catalytic ozonation with MgO nanocrystals. *Chem. Eng. J.*, 152(2009) 1-7.
- [14] F. Krika, O.F. Benlahbib, Removal of methyl orange from aqueous solution via adsorption on cork as a natural and low-cost adsorbent: equilibrium, kinetic and thermodynamic study of removal process. *Desalin. Water Treat.*, 53(2015) 3711-3721
- [15] X.S.Wang, J.P. Chen, Removal of the azo dye Congo red from aqueous solutions by the marine alga *Porphyra yezoensis* Ueda, *Clean Soil Air Water* 37 (2009)793-798
- [16] G. Bell (1997). Ecology and management of *Arundo donax*, and approaches to riparian habitat restoration in Southern California. In Brock, J. H., Wade, M., Pysek, P., and Green, D. (Eds.): *Plant Invasions: Studies from North America and Europe*. *Blackhuys Publishers, Leiden, The Netherlands*, 103-113.
- [17] LG. Angelini, L. Ceccarini, E. Bonari, Biomass yield and energy balance of giant reed (*Arundo donax* L.) cropped in central Italy as related to different management practices. *Eur. J. Agron.*, 22(2005) 375-389.
- [18] Lewandowski, JMO. Scurlock, E. Lindvall, M. Christou, The development and status of perennial rhizomatous grasses as energy crops in the US and Europe. *Biomass Bioenergy* 25(2003) 335-361.
- [19] A.A. Shatalov, H. Pereira, *Arundo donax* L. reed, new perspectives for pulping and bleaching. Part 4. Peroxide bleaching of organosolv pulps, *Bioresour. Technol.*, 96(2005) 865-872.
- [20] T.Vernersson, P.R. Bonelli, E.G. Cerrella, A.L. Cukierman, *Arundo donax* cane as a precursor for activated carbons preparation by phosphoric acid activation. *Bioresour. Technol.*, 8 (2002) 95-104.
- [21] G. Mavrogianopoulos, V. Vogli, S. Kyritsis, Use of wastewater as a nutrient solution in a closed gravel hydroponic culture of giant reed (*Arundo donax*). *Bioresour. Technol.*, 82(2002) 103-107.
- [22] H. Deng, Z.H. Ye, M.H. Wong, Accumulation of lead, zinc, copper and cadmium by wetland plant species thriving in metal-contaminated sites in China. *Environ. Pollut.*, 132(2004) 29-40.
- [23] H.L. Song, L. Liang, K.Y. Yang, Removal of several metal ions from aqueous solution using powdered stem of *Arundo donax* L. as a new biosorbent. *Chem. Eng. Res. Des.*, 92(2014) 1915-1922.
- [24] LS. Balistrieri, J.W. Murray, The surface chemistry of goethite ( $\alpha$ -FeOOH) in major ion seawater. *Am. J. Sci.*, 281(1981) 788-806.
- [25] SL.Goertzen, K.D. Theriault, AM Oickle, AC. Tarasuk, HA. Andreas, Standardization of the Boehm titration. Part I. CO<sub>2</sub> expulsion and endpoint determination, *Carbon* 48(2010) 1252-1261.
- [26] S. Lagergren, About the theory of so-called adsorption of soluble substances, *Handl.*, 24(1898) 1-39.
- [27] YS. Ho, MC. Kay, Pseudo-second-order model for sorption processes. *Process Biochem.*, 34(1999) 451-465.
- [28] WJ. Weber, JC. Morris, Kinetics of adsorption on carbon from solution, *J Sanit Eng Div.*, 89(1963) 31-59.
- [29] J. Eastoe, JS. Dalton, Dynamic surface tension and adsorption mechanisms of surfactants at the air J.S water interface. *Adv. J. Colloid Interface Sci.*, 85(2000) 103-144.
- [30] L.B.L. Lim, N. Priyantha, C.H. Ing, M.K. Dahri, D.T.B. Tennakoon, T. Zehra, M. Suklueng, *Artocarpus odoratissimus* skin as a potential low-cost biosorbent for the removal of methylene blue and methyl violet 2B, *Desalin. Water Treat.*, 53(2013) 964-975.
- [31] Y.S. Al-Degs, MI. El-Barghouthi, AH. El-Sheikh, GM. Walker, Effect of solution pH, ionic strength, and temperature on adsorption behavior of reactive dyes on activated carbon. *Dyes and Pigments* 77(2008) 16-23.
- [32] M.K. Dahri, M.R.R. Kooh, L.B.L. Lim, Application of *Casuarina quisetifolia* needle for the removal of methylene blue and malachite green dyes from aqueous solution. *Alexandria Engineering Journal* , 54(2015) 1253-1263
- [33] M.M. Abd El- Latif, A.M. Ibrahim, Adsorption, kinetic and equilibrium studies on removal of basic dye from aqueous solutions using hydrolyzed Oak sawdust. *Desalin. Water Treat.*, 6(2009) 252-268.
- [34] S. Kazemi, P. Biparva, E. Ashtiani, *Cerastoderma lamarcki* shell as a natural, low cost and new adsorbent to removal of dye pollutant from aqueous solutions: Equilibrium and kinetic studies. *Ecol. Eng.*, 88(2016) 82-89.
- [35] Y.Hu, T. Guo, X. Ye, Q. Li, M. Guo, H. Liu, Z.Wu, Dye adsorption by resins: effect of ionic strength on hydrophobic and electrostatic interactions. *Chem. Eng. J.*, 228(2013) 392-397.
- [36] M.K. Dahri, M.R.R. Kooh, L.B.L. Lim, Water remediation using low cost adsorbent walnut shell for removal of malachite green: equilibrium, kinetics, thermodynamic and regeneration studies, *J. Environ. Chem. Eng.*, 2(2014), 1434-1444.
- [37] M. Rathod, K. Mody, S. Basha, Efficient removal of phosphate from aqueous solutions by red seaweed, *Kappaphycus alvarezii*. *Journal of Cleaner Production*, 84(2014) 484-493.

- [38] Ö. Dülger, F. Turak, K. Turhan, M. Özgür. Sumac Leaves as a Novel Low-Cost Adsorbent for Removal of Basic Dye from Aqueous Solution. Hindawi Publishing Corporation, *Analytical Chemistry, 2013* (2013)9.
- [39] S. Sener, Use of solid wastes of the soda ash plant as an adsorbent for the removal of anionic dyes: Equilibrium and kinetic studies. *Chem. Eng. J.*, 138(2008) 207-214.
- [40] N. Dizge, C. Aydiner, E. Demirbas, M. Kobya, S. Kara, Adsorption of reactive dyes from aqueous solutions by fly ash: kinetic and equilibrium studies. *J. Hazard. Mater.*, 150(2008) 737-746.
- [41] H. Mittal, SB. Mishra, Gum ghatti and Fe<sub>3</sub>O<sub>4</sub> magnetic nanoparticles based nanocomposites for the effective adsorption of rhodamine B. *Carbohydr. Polym.*, 101(2014) 1255-1264.
- [42] M.N. Idris, M.A. Ahmad, Adsorption equilibrium of malachite green dye onto rubber seed coat based activated carbon. *Int. J. Basic App. Sci.* 11(2011) 38-43.
- [43] Langmuir, The adsorption of gases on plane surfaces of glass, mica and platinum. *J. Am. Chem. Soc.*, 40(1918) 1361-1368.
- [44] H. Freundlich, Adsorption in solution. *Phys. Chem. Soc.* 40(1906) 1361-1368.
- [45] M.J. Temkin, V. Pyzhev, Kinetics of ammonia synthesis on promoted iron catalysts. *Acta Physicochem.*, 2(1940) 217-222.
- [46] M.M. Dubinin, L.V. Radushkevich, Equation of the characteristic curve of activated charcoal. *Chem Zent.*, 1(1947) 875-889.
- [47] A.P. Meneghel, A.C.J. Gonçalves, F.Rubio, D.C. Dragunski, C.A. Lindino, L. Strey, Biosorption of cadmium from water using moringa (*Moringa oleifera* Lam.) seeds. *Water Air Soil Pollut.*, 224(2013) 1383-1396.
- [48] G. Annadurai, RS. Juang, D.J. Lee, Use of cellulose based wastes for adsorption of dyes from aqueous solutions. *J. Hazard. Mater.* 92(2002)263-274.
- [49] T. Zehra, N. Priyantha, L.B.L. Lim, Removal of crystal violet dye from aqueous solution using yeast-treated peat as adsorbent: thermodynamics, kinetics, and equilibrium studies. *Environ. Earth. Sci.*, 75(2016) 375.
- [50] H. Ali, S.K. Muhammad, Biosorption of crystal violet from water on leaf biomass of *Calotropis procera*. *J. Environ. Sci. Technol.*, 1(2008) 143-150.
- [51] B.K. Suyamboo, R.S. Perumal, Equilibrium, thermodynamic and kinetic studies on adsorption of a basic dye by *Citrullus lanatus* rind. *Iran. J. Energy Environ.* 3(2012) 23-24.
- [52] S. Hamidzadeh, M. Torabbeigi, SJ. Shahtaheri, Removal of crystal violet from water by magnetically modified activated carbon and nanomagnetic iron oxide. *J. Environ. Health Sci. Eng.*, 1(2015) 8-15.
- [53] M.A. Shouman, S.A. Khedr, A.A. Attia, Basic Dye Adsorption on low cost biopolymer: kinetic and equilibrium studies. *J. App. Chem.*, 2(2012) 27-36.
- [54] M.R. Kulkarni, T. Revanth, A. Acharya, P. Bhat. Removal of Crystal Violet dye from aqueous solution using water hyacinth: Equilibrium, kinetics and thermodynamics study. *Resour. Efficient Technol.*, 3(2017) 71-77.
- [55] M.J. Jaycock, GD. Parfitt, Chemistry of Interfaces, *Ellis Horwood Ltd., Onichester*, 1981.